



# CD24 is a novel target of chimeric antigen receptor T cells for the treatment of triple negative breast cancer

Peiwei Yang<sup>2,3</sup> · Fan Yu<sup>2,5</sup> · Zheng Yao<sup>2,3</sup> · Xu Ding<sup>4</sup> · Hanmei Xu<sup>2,3</sup> · Juan Zhang<sup>1,3</sup>

Received: 29 November 2022 / Accepted: 28 June 2023 / Published online: 7 July 2023  
© The Author(s), under exclusive licence to Springer-Verlag GmbH Germany, part of Springer Nature 2023

## Abstract

Triple negative breast cancer (TNBC) is a subtype of breast cancer with the highest degree of malignancy and the worst prognosis. The application of immunotherapy for TNBC is limited. This study was to verify the potential application of chimeric antigen receptor-T cells (CAR-T cells) targeting CD24 named as 24BBz in treatment of TNBC. 24BBz was constructed by lentivirus infection and then was co-culture with breast cancer cell lines to evaluate the activation, proliferation and cytotoxicity of engineered T cells. The anti-tumor activity of 24BBz was verified in the subcutaneous xenograft model of nude mice. We found that CD24 gene was significantly up-regulated in breast cancer (BRCA), especially in TNBC. 24BBz showed antigen-specific activation and dose-dependent cytotoxicity against CD24-positive BRCA tumor cells in vitro. Furthermore, 24BBz showed significant anti-tumor effect in CD24-positive TNBC xenografts and T cells infiltration in tumor tissues, while some T cells exhibited exhaustion. No pathological damage of major organs was found during the treatment. This study proved that CD24-specific CAR-T cells have potent anti-tumor activity and potential application value in treatment of TNBC.

**Keywords** CD24 antigen · CAR-T cell therapy · Solid tumor · TNBC

---

Peiwei Yang and Fan Yu have contributed equally to this paper.

✉ Hanmei Xu  
xuhanmei6688@126.com

✉ Juan Zhang  
zhangjuan@cpu.edu.cn

<sup>1</sup> Antibody Engineering Laboratory, Department of Molecular Biology, School of Life Science and Technology, China Pharmaceutical University, Nanjing 210009, People's Republic of China

<sup>2</sup> The Engineering Research Center of Synthetic Polypeptide Drug Discovery and Evaluation, China Pharmaceutical University, Nanjing 210009, Jiangsu Province, People's Republic of China

<sup>3</sup> State Key Laboratory of Natural Medicines, Ministry of Education, China Pharmaceutical University, 639 Longmian Avenue, Jiangning District, Nanjing City 210009, Jiangsu Province, People's Republic of China

<sup>4</sup> Department of Oral and Maxillofacial Surgery, Affiliated Hospital of Stomatology, Nanjing Medical University, Nanjing 210029, People's Republic of China

<sup>5</sup> Nanjing Anji Biological Technology Co., LTD, Nanjing 210033, People's Republic of China

## Introduction

Breast cancer (BRCA) is the most common cancer in women in the world [1]. Triple negative breast cancer (TNBC) is a subtype of breast cancer in which estrogen receptor (ER), progesterone receptor (PR) and proto-oncogene HER2 are negative according to pathological examination. The five-year survival rate is no more than 11% for TNBC patients in advanced stages [2–4]. Except for conventional chemotherapy and radiotherapy, only one ADC targeting TROP2 has been approved for clinical use [5–7]. Although immunotherapy has shown promising results in various types of tumors, its application for TNBC is limited. Therefore, it is urgent to find a new immunotherapy that can effectively improve the prognosis of TNBC patients.

Cluster of differentiation 24 (CD24) is an advanced glycosylated cell surface protein, which is highly expressed on many kinds of tumor cells, such as BRCA, ovarian cancer, cervical cancer, and oral mucosal melanoma [8–10]. Weissman et al. proved that CD24 is an innate immune checkpoint in BRCA and ovarian cancer which contributed to tumor cells escaping from the clearance of macrophages [11]. In TNBC, CD24 has been proved to promote tumor growth by activating Src kinase through the lipid raft [12].

The overexpression of CD24 is significantly correlated with more advanced pathological stage, shorter survival and is more likely to resistant to taxane-based treatment in TNBC patient [13–15]. In addition, CD24 is rarely found expressing on normal tissues, making it a preferable antigen for target therapy [16].

Chimeric Antigen Receptor-T cell (CAR-T cell) therapy is considered to be one of the most promising directions in cancer immunotherapy. CD24 as a promising target has been employed to redirect CAR-T cells to tumor cells. Maliar A et al. have demonstrated anti-CD24 CAR T cell therapy was effective in inhibiting tumor growth and metastasis in human pancreatic adenocarcinoma xenografts in mice [17]. Another study has constructed a bispecific BCMA-CD24 CAR-T cell and showed this novel CAR-T cell yielding near-complete tumor clearance for multiple myeloma cells in mice xenografts model [18]. However, the antibody employed in CD24 CAR-T cells in both of the studies mentioned above is mouse scFv SWA11. To date, no humanized CD24 scFv have been used to construct CAR-T cells. In addition, no studies have been reported to explore CD24-targeting CAR-T cells in triple-negative breast cancer.

In this study, we employed a humanized CD24 scFv which engineered in our previous study [19] to constructed a second-generation CAR- T cells 24BBz. We proved that 24BBz was able to be specifically activated in vitro, produce cytotoxicity and inhibit tumor growth in vivo. All these results suggested that CD24-CAR-T therapy may be a promising approach for the treatment of TNBC and other tumors with high expression of CD24.

## Methods and materials

### CD24 expression analysis in database

The Gene Expression Profiling Interactive Analysis (GEPIA) tool was used to analyze CD24 expression level from various human tumors and matched healthy tissues. The data are presented in a dot plot with y-axis showing as the  $\text{Log}_2$  (TPM + 1) scale. Next, the CD24 expression profiles in different subtypes of BRCA were analyzed in UALCAN database, using TCGA breast invasive carcinoma dataset. The survival curves (OS, RFS and DMFS) were presented by Kaplan–Meier plotter with the default parameters of database. Breast cancer scRNA-seq data were downloaded from the TISCH website (GSE176078). The data were read using the Read10X\_h5 function, and a Seurat object was constructed using Seurat (V 4.3.0). Cell subtypes were annotated using marker genes provided by the TISCH website. Expression levels of CD24 in different cell subtypes were visualized using ggplot2.

### Cell culture

MDA-MB-231, MDA-MB-468, T47D, BT474 and HEK-293T cells were obtained from ATCC. MDA-MB-231, MDA-MB-468 and HEK-293T cells were cultured in DMEM (high glucose) medium at 37 °C and 5% CO<sub>2</sub>, supplemented with 10% FBS (Biological Industries, Israel), 100 U/mL penicillin and 100 µg/mL streptomycin. T47D and BT474 cells were cultured in RPMI 1640 medium (Hyclone) at 37 °C and 5% CO<sub>2</sub>, supplemented with 15% FBS, 100 U/mL penicillin and 100 µg/mL streptomycin.

### Construction and production of lentivirus vector

CD24 CAR consists of CD8 $\alpha$  signal peptide, V<sub>H</sub>-(G<sub>4</sub>S)<sub>3</sub>-V<sub>L</sub>, CD8 hinge, CD8 transmembrane region, 4-1BB intracellular costimulatory signal region, CD3 $\zeta$  intracellular signal, T2A and truncated EGFR (EGFRt) fragment [20]. The CD24 scFv sequence was provided by Professor Zhang of China Pharmaceutical University, and the other gene segments were found in the National Biotechnology Information Center (NCBI). The corresponding DNA sequences were obtained from iCARTaB BioMed after codon optimization and then ligated into the pLV-puro vector via *Cla* I and *Xba* I. In addition, a control vector was constructed which only had the EGFRt fragment, named Mock.

HEK-293T cells were used to produce lentiviral particles. 20 µg of pLV-puro, psPAX2 and pMD.2G (4:2:1) were transfected into HEK-293 T cells using EZ Trans (SHANGHAI LIFE iLAB TECHNOLOGY). After 24 h and 48 h, the supernatant was collected, filtered with a 0.45-µm filter and centrifuged at 20,000 × g for 120 min. Finally, the lentiviral particles were resuscitated in 200 µL medium and stored at –80 °C.

### Transfection and identification of CAR-T cells

Fresh blood was obtained from healthy volunteers with the approval of the Ethics Committee of China Pharmaceutical University. Human peripheral blood mononuclear cells (PBMC) were isolated by Ficoll density gradient centrifugation (P8900; Solarbio). CD3<sup>+</sup> T cells were enriched by magnetic beads separation (Miltenyi Biotec) and activated by human CD3/CD28 beads (Life Technologies) for 48 h. Then, the activated T cells were collected and cultured in RPMI 1640 culture medium (Hyclone) at 37°C and 5% CO<sub>2</sub>, supplemented with 10% FBS, 100 U/mL penicillin, 100 µg/mL streptomycin and other growth factors including MEM non-essential amino acid solution (Gibco), sodium pyruvate (Gibco), L-glutamine (Gibco) and 0.1% 2-mercaptoethanol (Gibco). In addition, 100 U/mL human interleukin 2

(IL-2, PeproTech) was added to promote the expansion of T cells.  $1 \times 10^6$  activated T cells were collected and added to a 24-well plate in the presence of fresh culture medium supplemented with 6  $\mu\text{g}/\text{mL}$  polybrene (Sigma-Aldrich). The lentivirus was added at MOI= 10, and then, the mixture was centrifuged at 1200 g for 90 min at 31 °C and incubated overnight at 5% CO<sub>2</sub> and 37 °C. The next day, the virus fluid was discarded, and the engineered T cells were cultured in RPMI 1640 medium supplemented with 10% FBS, 100 U/mL penicillin, 100  $\mu\text{g}/\text{mL}$  streptomycin, 300 U/mL human IL-2 and other necessary growth factors. On the fifth day after transfection, the expression of EGFRt, and the relative CD4/CD8 ratio and memory phenotype of engineered T cells were evaluated by flow cytometry. The successfully constructed CAR engineered T cells were named 24BBz.

### Flow cytometry

EGFR-PE, CD24-PE, CD69-APC, CD25-PE, CD4-PE, CD8-APC, PD-1-BV421, CD62L-APC-CY7, CD45RA-FITC and CD3-FITC antibodies were purchased from Biolegend. For flow cytometry analysis, all cells were collected by centrifugation at 4 °C and washed three times by pre-chilled PBS buffer. Then, the detection antibody was added into the cell suspension and incubated at 4 °C for 30 min in the dark. The cells were detected on the CytoFLEX after washed three times with pre-cooled PBS buffer and filtered through a 300-mesh nylon mesh; the data were processed through Flowjo V10.

### Cytotoxicity and cytokine release assays

Effector cells and target cells were co-cultured in 96-well cell culture plates at the effector–target ratio of 1:1, 2:1, 4:1 and 8:1 for 24 h, and the LDH cytotoxicity assay kit (Beyotime) was used to detect the lactate dehydrogenase (LDH) level in the co-incubation supernatant, which can characterize the cytotoxic effect of effector cells. The absorbance at 490 nm of each well was recorded using a Multiskan FC tablet reader (Thermo Science), and the cytotoxicity was calculated as the following formula: cytotoxicity (%) = (co-incubation lysis-effector cells spontaneous lysis-target cells spontaneous lysis)/(target cell maximum lysis-target cell spontaneous lysis)  $\times$  100%.

Supernatant was collected after effector cells and target cells were co-incubated 24 h in a 96-well plate at a ratio of 2:1 and IL-2 and IFN- $\gamma$  were measured by using ELISA kit (MultiSciences, Hangzhou, China).

### Detection of cell proliferation and apoptosis

On day 0, a certain number of effector cells were stained with the prepared Cell Trace™ CFSE stain reagent

(ThermoFisher) according to the instruction manual and incubated with target cells for three days. Fluorescence intensity of effector cells on day 0 and day 3 was recorded by flow cytometry, and the dilution ratio was used to evaluate cell proliferation.

After 7 days of in vitro expansion, T cells were collected and cell apoptosis was determined by flow cytometry via an Annexin V-FITC/PI apoptosis detection kit (MultiSciences, Hangzhou, China).

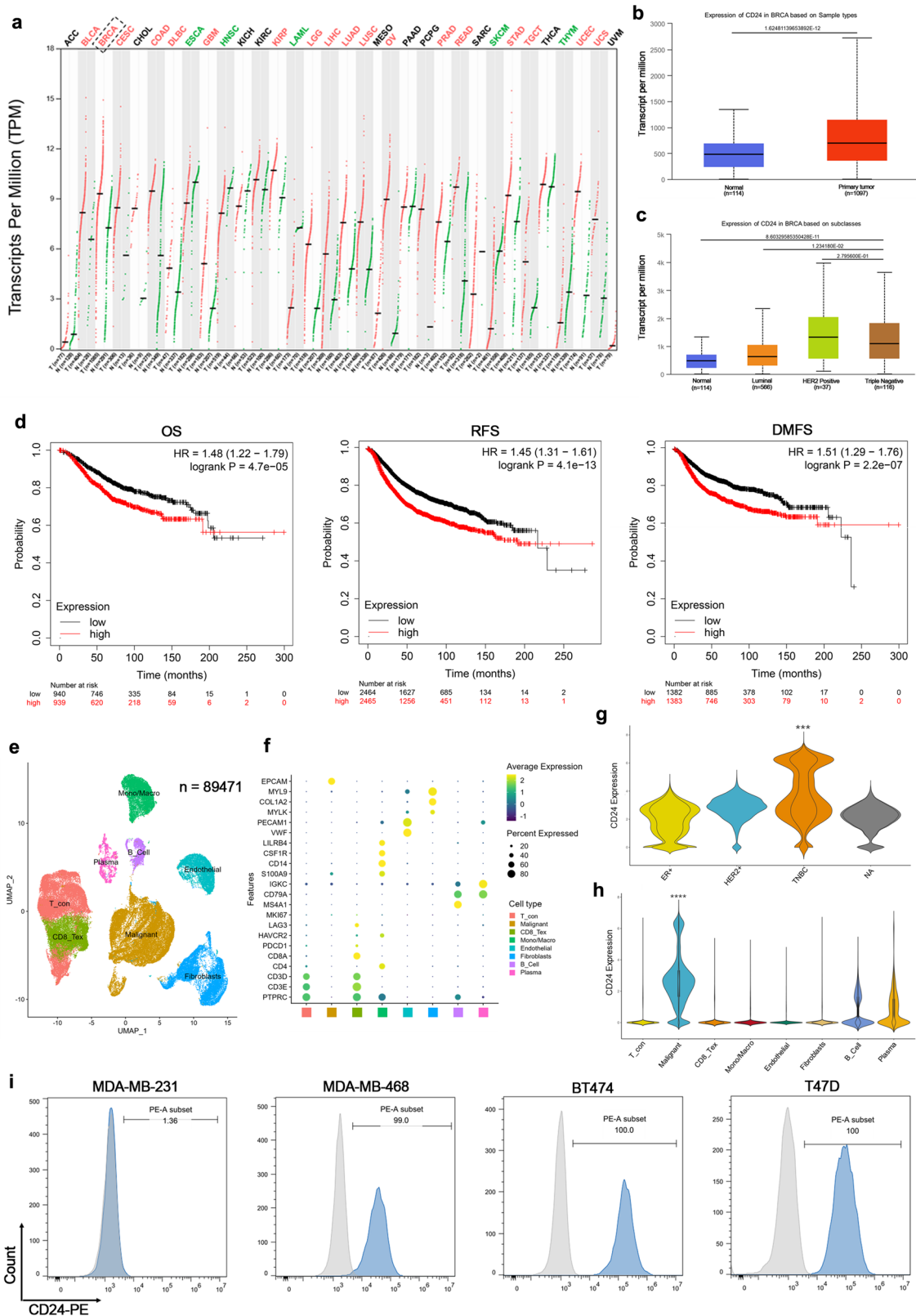
### In vivo experiments

In our study, the BALB/c female nude mice (4–6 weeks old) were purchased from the Animal Center of Yangzhou University and raised in the SPF animal laboratory. All procedures were conducted in conformity with guidelines of the China Pharmaceutical University.  $3 \times 10^6$  MDA-MB-231 cells and  $1 \times 10^7$  MDA-MB-468 cells were inoculated in the mammary fat pads per mouse, respectively, on day 0. When the tumor established (Volume > 50 mm<sup>3</sup>), randomize grouping ( $n = 5/\text{group}$ ) was performed.  $1 \times 10^7$  24BBz or Mock T cells were administered by intravenous or peritumoral injection (i.v or p.t). The survival status of the mice was observed in real time, and the tumor volume of the mice was measured once a week. The tumor volume calculation formula: tumor volume (mm<sup>3</sup>) = (length  $\times$  width<sup>2</sup>)/2. Peripheral blood from mice was collected and T cell proportion was quantified for the collected blood samples 7 days after 24BBz treatment. After lysis of red blood cells in peripheral blood, CD3-FITC antibody was added and incubated for 30 min at 4 °C in the dark. The detection was performed using CytoFLEX. The positive cell population was determined by detecting CD3 + T cells in PBMCs using a gating strategy as shown in Figure S3. On the 27 th and 43 th day, the mice were administered euthanasia. The weight of the tumor tissues was measured.

### IHC and HE staining analysis

The tumor, heart, liver, spleen, lung and kidney tissues were fixed overnight in paraformaldehyde (4%) after euthanasia. The tissues were embedded in paraffin and cut into tissue sections with a thickness of 5  $\mu\text{m}$ . The tissue sections were then staining by Hematoxylin and Eosin Staining Kit.

Otherwise, tumor tissue sections were prepared for immunohistochemical (IHC) detection and details were as follows: Paraffin sections were deparaffinized and hydrated in xylene and graded alcohol, and then, antigen retrieval was performed for 20 min in Tris–EDTA solution of pH 9.0 at 98 °C. The sections were cooled, rinsed with 1  $\times$  PBS and incubated in a 3% H<sub>2</sub>O<sub>2</sub> solution for 10 min. For blocking, the tissue sections were incubated in goat serum for 1 h and then incubated with rabbit anti-human CD3 antibody (CST,



1:100), rabbit anti-human PD-1 antibody, rabbit anti-human GzmB antibody and rabbit anti-human IFN- $\gamma$  antibody at 4 °C overnight. The next day, the tissue sections were

incubated with solution of horseradish peroxidase-labeled secondary antibody (diluted at a ratio of 1:1000) for 1 h at room temperature. Finally, the sections were incubated in

**Fig. 1** Expression of CD24 in breast cancer **a** CD24 gene expression profile across tumor samples and paired normal tissues. **b** CD24 expression level of tumor or normal tissues in BRCA was analyzed. **c** CD24 expression level in different BRCA types was analyzed. **d** Kaplan–Meier analysis indicated that patients with high CD24 expression level suffered significantly worse outcomes (OS, RFS and DMFS). **e** A single-cell clustering plot was generated, and a total of 89471 cells were analyzed. **f** Dot plots showing the expression of major cell markers in each cell type. **g** Violin plots depicting the expression of CD24 in malignant epithelial cells across different subtypes of tumor patients. **h** Violin plots depicting the expression of CD24 in different cell subtypes were generated specifically for TNBC patients. **i** The expression of CD24 was detected in several kinds of human breast cancer cells by flow cytometry analysis

DAB substrate solution for 2–5 min, counterstained with hematoxylin, rinsed with water, and dehydrated in graded alcohol and xylene. Coverslips were mounted with neutral resin, and images were acquired on microscope (Olympus).

### Statistical analysis

All the data were displayed as the mean  $\pm$  SD and were performed by using two-tailed Student's *t* test. The GraphPad 8.0 software was applied for statistical analysis.  $P < 0.05$  was considered statistically significant.

## Results

### CD24 expression in BRCA

Gene expression analysis in GEPIA revealed that CD24 gene was up-regulated in most types of cancer with the highest expression in BRCA (Fig. 1a). The data in UALCAN indicated that the expression of CD24 in tumor tissues was significantly higher than that in normal tissues. Its expression was further elevated in the HER2 positive and triple negative subtype, while there was no expression difference between these two types (Fig. 1b, c). The survival analysis showed that the high expression of CD24 was related to the worse survival rate (including OS, RFS and DMFS) of BRCA patients (Fig. 1d). Kwon et.al also demonstrated that high CD24 expression is independently associated with poorer survival in luminal A and TNBC subtypes [13]. In addition, single-cell sequencing analysis on public data of breast cancer tissues was performed. A total of 89,741 cells were analyzed, and 8 cell subtypes were defined (Fig. 1e, f). Analysis of the malignant epithelial cell subtype revealed that the expression level of CD24 in TNBC group's tumor cells was significantly higher than tumor cells in other subtypes (Fig. 1g). Furthermore, further analysis of TNBC patients showed that CD24 was mainly expressed in malignant epithelial cells and almost not expressed in T lymphocytes (Fig. 1h). Finally, we examined CD24 expression in

four human breast cancer cells by flow cytometry. T47D, BT474 and MDA-MB-468 highly expressed CD24 while no expression of CD24 in MDA-MB-231 (Fig. 1i).

### Characterization of 24BBz

To redirect T cells to CD24 expressed tumor cells, a second-generation CAR vector, including CD24 scFv, was constructed. A truncated EGFR as a detecting marker was co-expressed with CAR separated by T2A sequence (Fig. 2a). 15 days after transduction, engineered T cells reached about 200-fold expansion during in vitro culture (Fig. 2b). The transduction efficiency of Mock T and 24BBz represented by EGFRt were 41% and 52%, respectively, as detected by flow cytometry analysis (Fig. 2c). The status of T cells, including CD4/CD8 ratio, memory phenotype, and apoptosis level, was analyzed by flow cytometry after transfection. The results showed that there is no difference in the proportions of CD8+ and CD4+ T cells in untransduced T cells, Mock T and 24BBz cells (Fig. 2d), but more engineered T cells were switched to the effector memory phenotype (CD62L<sup>−</sup>CD45RA<sup>−</sup>) (Figure e, Supplementary Fig. 1). Furthermore, after seven days of in vitro expansion, no obvious apoptotic signal was observed in each group (Fig. 2f). These results supported the successful construction of 24BBz.

### 24BBz shows a strong anti-tumor activity against breast cancer cells in vitro

To examine the cytotoxicity of 24BBz against CD24+ tumor cells, the LDH releasing assays were performed. The results showed that the lytic activity of 24BBz on CD24-positive cells was enhanced with the increase of E:T ratio and was significantly stronger than that of Mock T. In contrast, all effector cells produced slight cytotoxicity at each E:T ratio against CD24-negative MDA-MB-231 cells (Fig. 3a).

To find out the activation of 24BBz, the surface biomarkers, such as CD25 and CD69, were detected by cytometry. The results indicated that the up-regulation of CD25 and CD69 expression on 24BBz when incubated with CD24-positive tumor cells (T47D, BT474, MDA-MB-468) compared with Mock T. No remarkable CD25 and CD69 expression changes were found on Mock T and 24BBz against CD24-negative MDA-MB-231 cells (Fig. 3b, c). T cells made significant proliferation and secreted multiple cytokines after activation. Therefore, the proliferation of 24BBz and the secretion of IL-2 and IFN- $\gamma$  were examined as well. The carboxy fluorescein diacetate succinimidyl ester (CFSE)-based proliferation assay showed a higher proliferation of 24BBz than that of Mock T when incubated against CD24-positive tumor cells, whereas no difference in proliferation of 24BBz and Mock T when incubated against CD24-negative tumor



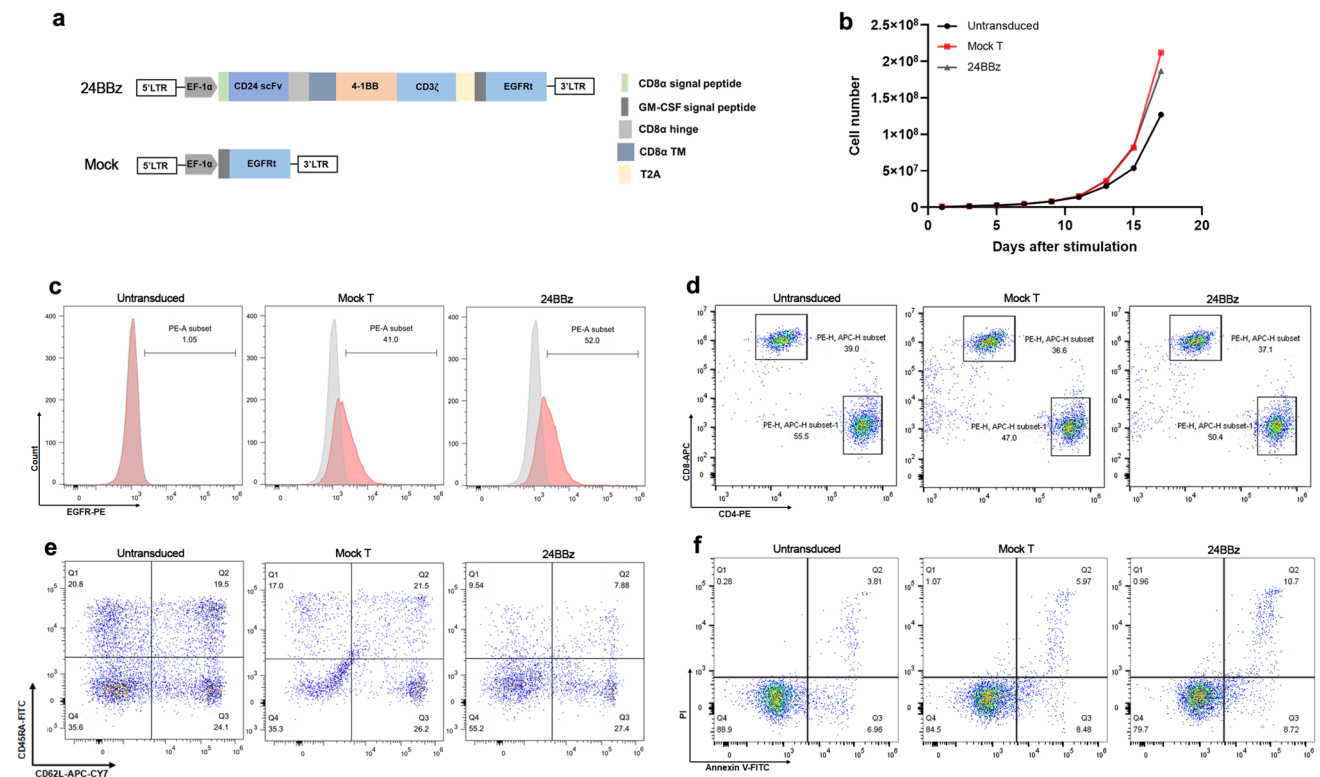


**Fig. 2** Construction and characterization of 24BBz **a** Schematic diagram of the CAR. **b** Expansion curve of engineered T cells cultured in vitro after stimulation. **c** Flow cytometry detection of EGFRt expression in engineered T cells to evaluate their transfection rate. **d** CD4<sup>+</sup> and CD8<sup>+</sup> engineered T cells were assessed by flow

cytometry. **e** T cell memory phenotypic analysis, TCM (CD45RA<sup>-</sup>/CD62L<sup>+</sup> central memory T cells), TEM (CD45RA<sup>-</sup>/CD62L<sup>-</sup> effector memory T cells). **f** The apoptosis level of T cells after 7 days of culture in vitro was detected by flow cytometry. (PI<sup>+</sup>/Annexin V<sup>+</sup> late apoptosis, PI<sup>-</sup>/Annexin V<sup>+</sup> early apoptosis)

cells (Fig. 3d). In addition, more IL-2 and IFN- $\gamma$  were produced by 24BBz than Mock T in the presence of CD24-positive tumor cells, while a little secretion of IL-2 and IFN- $\gamma$  in both 24BBz and Mock T were observed in the presence of CD24-negative tumor cells (Fig. 3e). Finally, to determine the exhaustion of T cells after stimulation, PD-1 expression was evaluated on 24BBz. Flow cytometry analysis showed that the expression of PD-1 was not apparently different among different groups (Fig. 3f). These results jointly proved that 24BBz can be specifically activated, kill target cells and sustain a favorable effector cytokine profile in vitro.

### 24BBz shows a strong anti-tumor activity on subcutaneous TNBC mouse models

In order to evaluate the in vivo anti-tumor activity of 24BBz, we selected two TNBC cell lines (MDA-MB-231 and MDA-MB-468 cells) to establish a xenograft tumor model and reinfused the 24BBz by intravenous or peritumoral injection (i.v. or p.t.). 28 days after treatment, the tumor volume of MDA-MB-468 xenograft in 24BBz/i.v. and 24BBz/p.t. was less than Mock T (Fig. 4a, b). There was also a lower tumor weight in 24BBz/i.v. and 24BBz/p.t. compared with Mock

T. But there was little apparent difference in tumor inhibition growth compared with 24BBz/i.v. and 24BBz/p.t. group (Fig. 4c). In contrast, no inhibition of MDA-MB-231 tumor growth was found in either Mock T or 24BBz treated groups at day 21 following T cell administration (Fig. 4d–f). In addition, no obvious weight change (Supplementary Fig. 2) and damage could be observed in major organs from each group in MDA-MB-468 or MDA-MB-468 xenograft model (Fig. 4g). These results revealed that 24BBz was able to eliminate CD24-positive TNBC xenografts in vivo with little side effects.

### 24BBz shows well infiltration and effector function in vivo

Previous studies have found that persistence of CAR-T cells was highly correlated with therapeutic effect [21] so we detected CD3<sup>+</sup> T cell in the peripheral blood of mice at day 7 after treatment. Flow cytometry analysis indicated that 24BBz had a better persistence in both i.v. group and p.t. group than Mock T, while a similar CD3<sup>+</sup> T cell proportion was found in 24BBz/i.v. and 24BBz/p.t. group in MDA-MB-468 xenograft model (Fig. 5a). No significant difference of T cell proportion

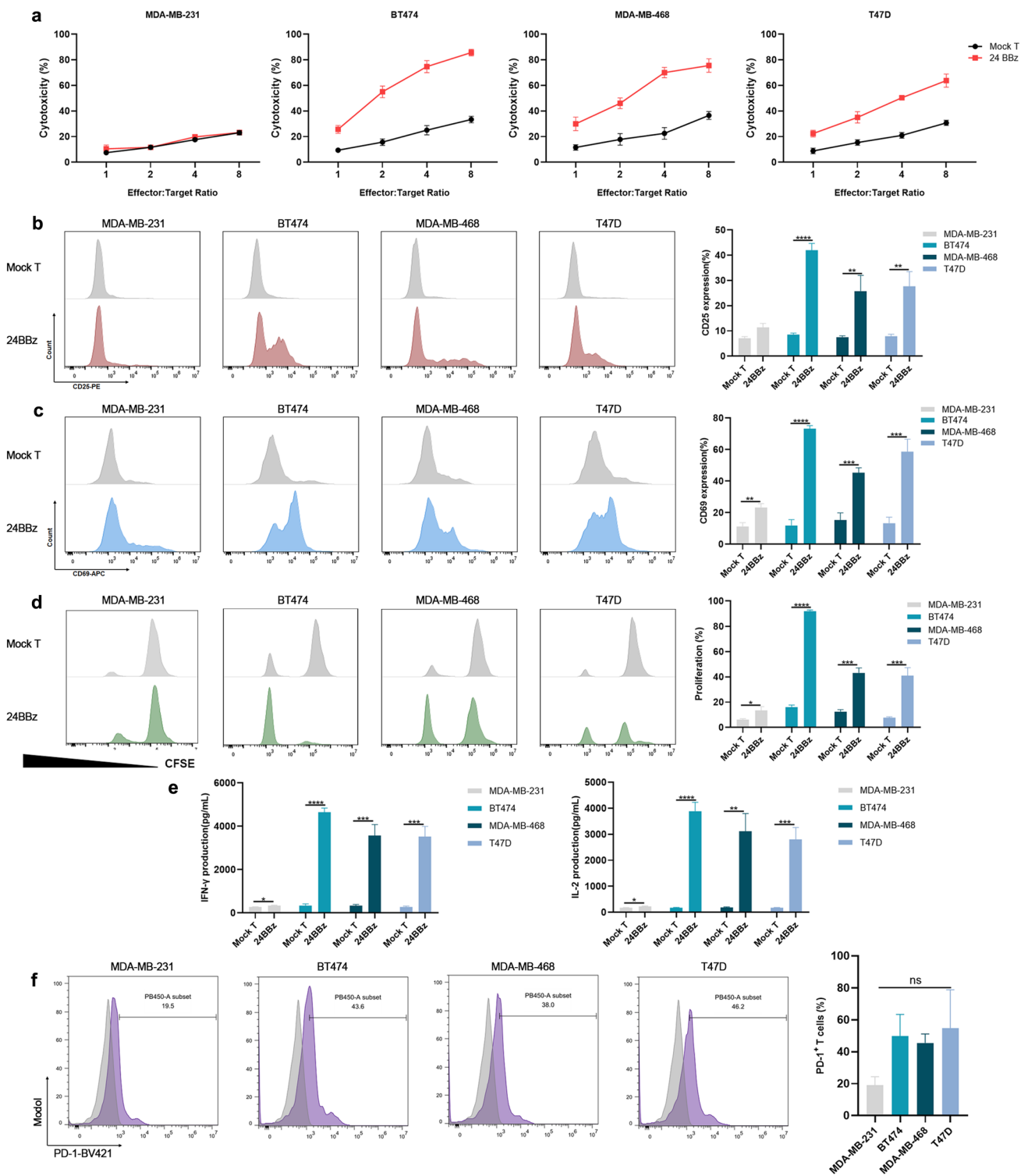


**Fig. 3** Antigen-specific activation and dose-dependent cytotoxicity of 24BBz against CD24 expressing tumor cell lines in vitro **a** lactate dehydrogenase (LDH) levels in the supernatants of different E: T co-culture systems were detected to characterize the lysis effect of 24BBz and Mock T on target cells. The expression of CD25 **b** and CD69 **c** on the surface of T cells was detected by flow cytometry after co-incubating with target cells for 24 h. **d** The engineered T cells

were stained with Cell Trace™ CFSE, and after three days of co-incubation, the proliferation ability was detected by flow cytometry. **e** 24 h after incubation of effector cells and target cells at ratio of 2:1, levels of IFN- $\gamma$  and IL-2 secreted by T cells were measured. **f** Flow cytometry analysis of the expression of PD-1 on the T cells after three days co-incubation. ( $n=3$ , error bars denote standard deviation, ns  $P>0.05$ , \* $P<0.05$ , \*\* $P<0.01$ , \*\*\* $P<0.001$ , \*\*\*\* $P<0.0001$ )

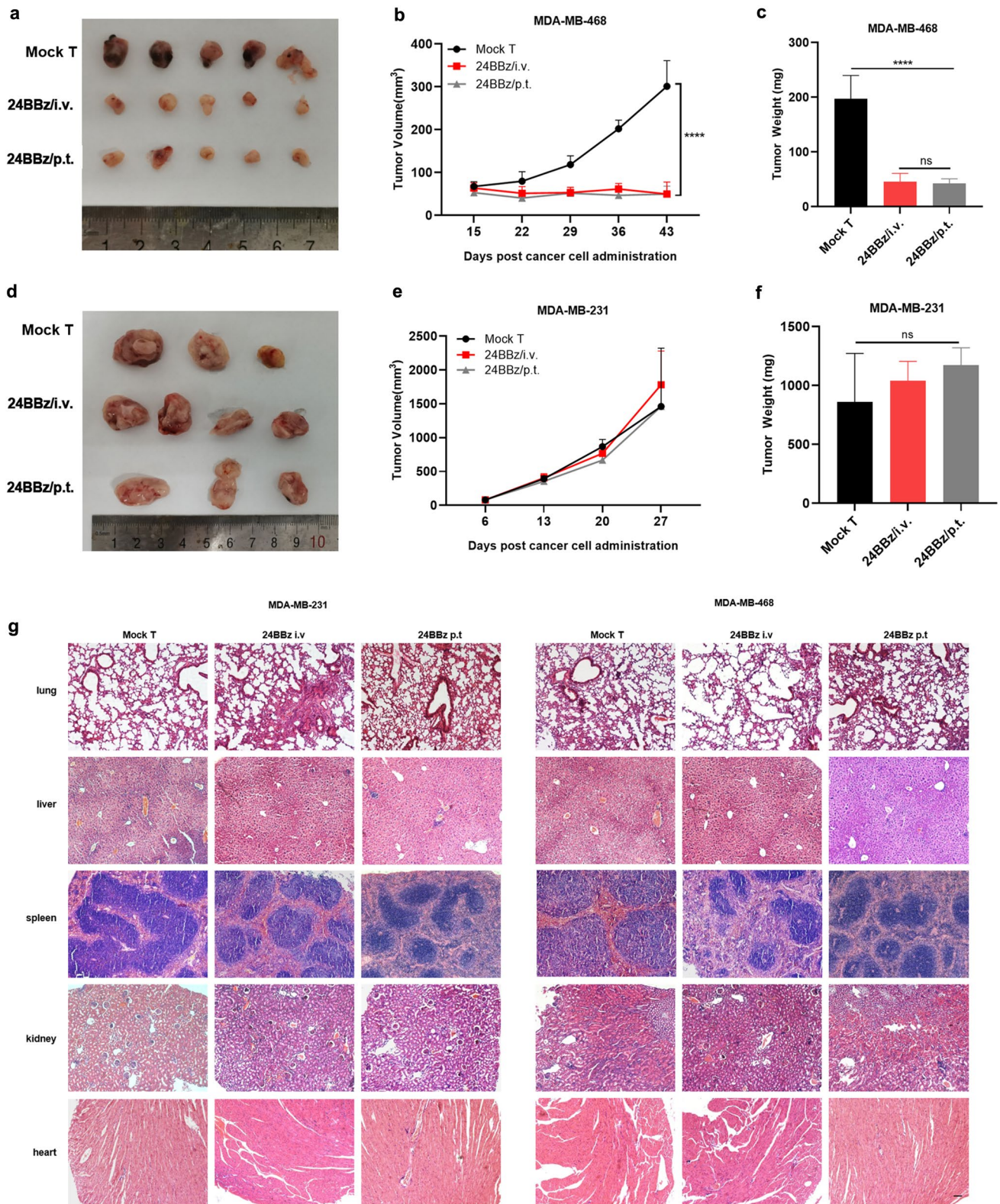


**Fig. 4** In vivo anti-tumor activities of 24BBz in TNBC bearing mice **a, d** The imaging of tumors in MDA-MB-231 bearing mice or MDA-MB-468 bearing mice treated with 24BBz/i.v., 24BBz/p.t. and Mock T. **b, e** Tumor volume quantification was monitored weekly. **c, f** The

weight of the tumors in each group was measured. **g** HE staining was performed to evaluate the pathological changes of heart, lung, liver, kidney and spleen tissues from each group ( $\times 100$ ). ( $n=5$ , error bars denote standard deviation,  $**P<0.01$ ,  $***P<0.001$ ,  $****P<0.0001$ )



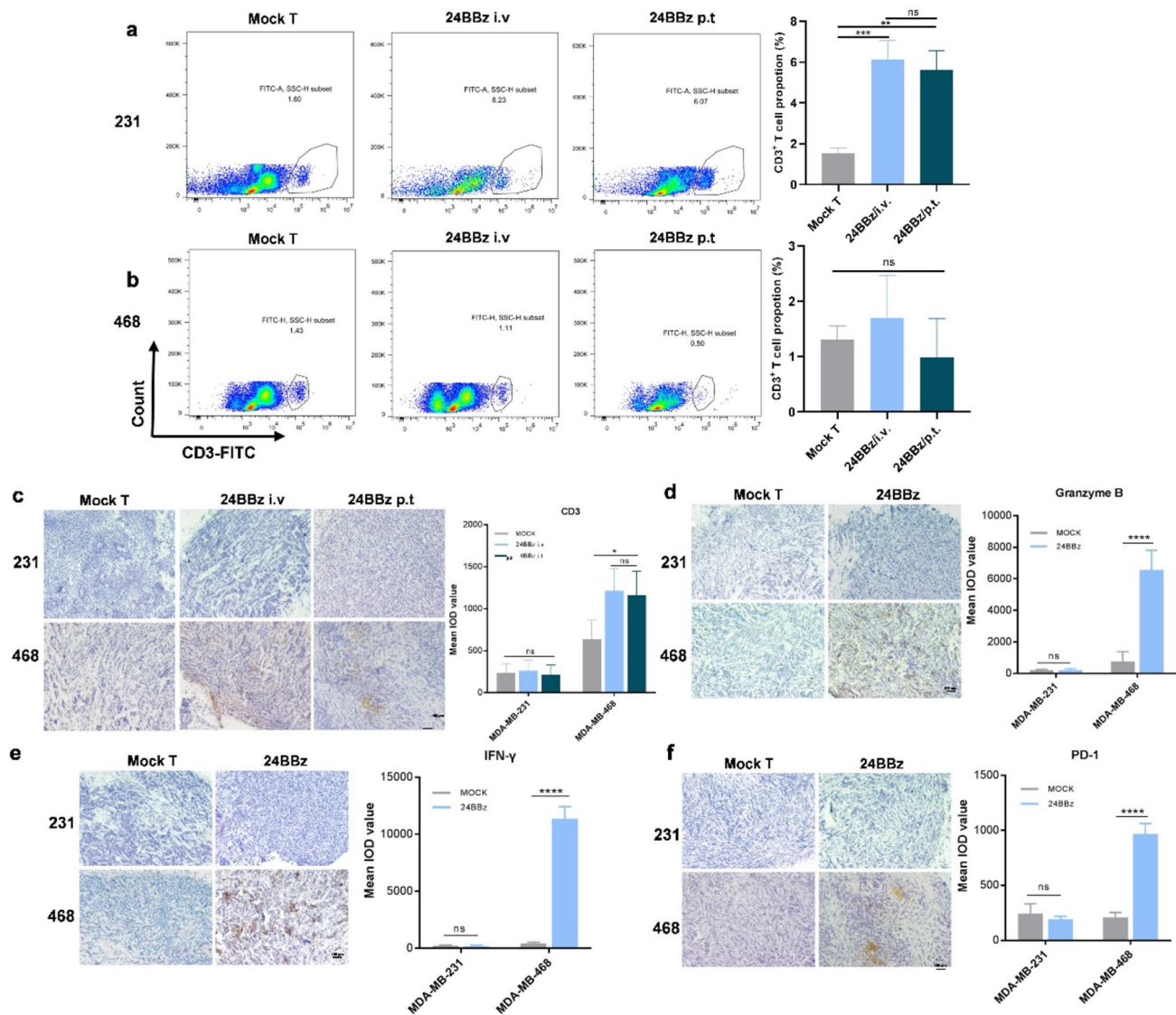


**Fig. 5** In vivo effector function of 24BBz **a, b** The proportion of CD3<sup>+</sup> T cells in peripheral blood of mice was detected by flow cytometry. **c** After intravenous and peritumoral administration of the treated cells, T cells infiltration in tumor tissue was analyzed by IHC. **d** Detection of the level of granzyme B secreted by T cells in tumor

tissues from i.v. group. **e** Detection of the level of IFN- $\gamma$  secreted by T cells in tumor tissues from i.v. group. **f** IHC analysis of the expression of PD-1 on the surface of infiltrating T cells in tumor tissues from i.v. group. ( $n=5$ , error bars denote standard deviation,  $*P<0.05$ ,  $**P<0.01$ ,  $***P<0.0001$ )

was found between Mock T, 24BBz/i.v. and 24BBz/p.t. group in MDA-MB-231 xenograft model (Fig. 5b). Next, the infiltration of T cell was detected by CD3 immunohistochemical staining. The results displayed that a greater number of T cells were infiltrated into tumor in 24BBz/i.v. and 24BBz/p.t. group than Mock T group in MDA-MB-468 xenograft model, which was consistent with the circulating T cells in the peripheral blood (Fig. 5c). Furthermore, the effector function of 24BBz in tumor was evaluated. The 24BBz-treated group in MDA-MB-468 xenograft model had the highest level of GzmB and IFN- $\gamma$  among all groups (Fig. 5d, e). However, highest PD-1 staining was also found in 24BBz-treated group

in MDA-MB-468 xenograft model among all groups, which may be related to the specific activation of 24BBz by CD24 antigen (Fig. 5f). These data suggested that the 24BBz could maintain in the peripheral blood, infiltrate into tumor tissue and exert anti-tumor activity in CD24-positive xenograft.

## Discussion

TNBC is a highly aggressive and fatal breast cancer subtype that has only surgery and chemotherapy for treatment [22]. CAR-T cells have made great breakthroughs in treatment

of a variety of hematological malignancies, including large B-cell lymphoma, multiple myeloma and acute lymphoblastic leukemia [23]. Various preclinical studies of CAR-T cells in solid tumor were also extensively explored. Although some CAR-T cells (targeting such as EGFR [24], EpCAM [25], c-MET [26], MUC1 [27], AXL [28], TROP2 [29]) have been validated in preclinical study for TNBC, little clinical breakthrough was found to date. In this study, we constructed a novel second-generation CAR, which could redirect T cells target to CD24 and cause well anti-tumor activity in CD24-positive breast cancer cells in vitro and CD24-positive TNBC xenograft in vivo.

Barkal et al. observed that the expression of CD24 was up-regulated in almost all tumor types through RNA sequencing data from the TARGET and TCGA databases [11]. Other studies also demonstrated CD24 is overexpressed in many tumors and is a suitable target for prognosis, diagnosis, and targeted therapy on various cancers [30]. In this work, RNA-sequencing data from GEPIA revealed highest expression level of CD24 in BRCA. Analysis in UALCAN indicated that CD24 expression in TNBC was further increased among different subtypes of BRCA. These evidences suggest that CD24 may be a potential target for CAR-T cell therapy against TNBC.

In our previous work, a CD24 specific monoclonal antibody was screened by hybridoma technology and confirmed that the CD24 scFv (G7S) has similar affinity and higher specificity to the commercial CD24 antibody (ML5) [31]. Then, a humanized antibody, named hG7-BM3, has been produced and proved to have the similar affinity parameters with the parental chimeric antibody G7S [19]. It has been reported that mouse scFv used in CAR-T cells could cause anaphylaxis [32]. Therefore, 24BBz redirected to CD24 was developed using hG7-BM3 scFv as the targeting moiety. Antigen-dependent activation of 24BBz was demonstrated by activation marker (CD25, CD69) expression, proliferation, and cytokine secretion in vitro. We also proved 24BBz could destroy CD24-positive BRCA cells and have little cytotoxicity against CD24-negative BRCA cells in vitro. In addition, 24BBz exhibited well tumor inhibition ability in CD24-positive TNBC xenograft mouse model.

The delivery of CAR-T cells may produce different curative effects. Lv et al. proved peritumoral delivery of MSLN CAR-T cell enhanced CAR-T cells infiltration into tumor tissue at the early stage and cause tumor regression [33]. It is indeed that regional CAR-T cell delivery could theoretically compensate for poor T-cell trafficking and tumor antigen specificity in solid tumor [34, 35]. In our study, the tumor control ability was evaluated by systemic i.v. administration or regional p.t. administration of 24BBz in TNBC xenograft mouse model. We found that 24BBz induced similar tumor regression in CD24-positive TNBC xenograft mouse model with the similar T cell persistence and infiltration in vivo.

We speculated that the difference between our results and those of Lv et al. was due to the discrepancy of tumor volume at the time of T cell reinfusion. A major factor resulting in the low response rate of CAR T cells in solid tumors is the extensive immunosuppressive microenvironment [36]. Multiple studies have elucidated that immune checkpoint receptor signaling may result in T-cell exhaustion, causing T cells to become incapacitated against tumor cells [37, 38]. Our study showed that the expression of PD-1 on 24BBz was up-regulated after co-incubation in vitro. Meanwhile, in the CD24-positive TNBC xenograft mouse model, immunohistochemical results showed significant PD-1 expression in the 24BBz treatment group, which may be an important factor limiting the further elimination of tumor cells by 24BBz. It was reported that the combination of CAR-T cell therapy and PD-1 blockade, such as nivolumab and pembrolizumab, has been applied to enhance the effectiveness of anti-tumor therapy in clinical trials [39]. In addition, some studies have tried to construct armored CAR-T cells to secrete PD-1 antibody [40], or used the CRISPR/Cas9 system to knock out the PD-1 receptor gene in CAR-T cells to improve the anti-tumor activity of CAR-T cells [41]. These modifications to 24BBz will be tested in future work to further improve its efficacy.

At present, the safety of CAR-T cells like “On-target, off-tumor effect” is a major concern for its clinical application [42, 43]. Due to the characteristics of CD24 antigen expression and the specificity of G7S, no tissue damage in major organs was found after 24BBz treatment. Additional toxicological studies will be conducted in future studies. In addition, previous research proved that targeting EGFRt with the IgG1 monoclonal antibody cetuximab could eliminate CD19 CAR-T cells both early and late after adoptive transfer [44], thus EGFRt as a “safety switch” co-expressed on the 24BBz could potentially prevent fatal side effect. This role of EGFRt will be also evaluated in our future study.

In conclusion, our study demonstrated the potent anti-tumor efficacy of 24BBz against CD24-positive TNBC cells in vitro and in vivo, suggesting that 24BBz could become a potential option for the clinical treatment of TNBC in future.

**Supplementary Information** The online version contains supplementary material available at <https://doi.org/10.1007/s00262-023-03491-7>.

**Authors' contributions** YPW, YF and YZ designed and performed the experiments, analyzed the data, created the figures and wrote the paper. DX collected the blood sample. ZJ and XHM conceived the idea, supervised the project, and edited the paper. All authors carefully read and approved the paper.

**Funding** This work was supported by the Project Program of State Key Laboratory of Natural Medicines (SKLNMZZ202219), the National Natural Science Foundation (NSFC81973223), the Fundamental Research Funds for the Central Universities (2632023GR08) and the Nanjing International Industry Technology Research and Development Cooperation Project (2021SX00000435-202100880).

**Data availability** Data are available on reasonable request.

## Declarations

**Conflict of interest** The authors declare that they have no known competing financial interests or personal relationships that could have appeared to influence the work reported in this paper.

**Ethical approval** Animal experiments were conducted in conformity with guidelines of the China Pharmaceutical University.

**Consent to participate** Fresh blood was obtained from healthy volunteers with the approval of the Ethics Committee of China Pharmaceutical University. Informed consent was obtained from all individual participants.

**Consent to publish** All authors and subjects in this study concur with the publish.

## References

- Loibl S, Poortmans P, Morrow M, Denkert C, Curigliano G (2021) Breast cancer. *Lancet* (London, England) 397(10286):1750–1769. [https://doi.org/10.1016/s0140-6736\(20\)32381-3](https://doi.org/10.1016/s0140-6736(20)32381-3)
- Bianchini G, De Angelis C, Licata L, Gianni L (2022) Treatment landscape of triple-negative breast cancer-expanded options, evolving needs. *Nat Rev Clin Oncol* 19(2):91–113. <https://doi.org/10.1038/s41571-021-00565-2>
- Hua Z, White J, Zhou J (2022) Cancer stem cells in TNBC. *Semin Cancer Biol* 82:26–34. <https://doi.org/10.1016/j.semcancer.2021.06.015>
- Garrido-Castro AC, Lin NU, Polyak K (2019) Insights into molecular classifications of triple-negative breast cancer: improving patient selection for treatment. *Cancer Discov* 9(2):176–198. <https://doi.org/10.1158/2159-8290.Cd-18-1177>
- He MY et al (2018) Radiotherapy in triple-negative breast cancer: current situation and upcoming strategies. *Crit Rev Oncol Hematol* 131:96–101. <https://doi.org/10.1016/j.critrevonc.2018.09.004>
- Nedeljković M, Damjanović A (2019) Mechanisms of chemotherapy resistance in triple-negative breast cancer-how we can rise to the challenge. *Cells*. <https://doi.org/10.3390/cells8090957>
- Jabbarzadeh Kaboli P et al (2022) Shedding light on triple-negative breast cancer with Trop2-targeted antibody-drug conjugates. *Am J Cancer Res* 12(4):1671–1685
- Kristiansen G et al (2003) CD24 expression is a new prognostic marker in breast cancer. *Clin Cancer Res* 9(13):4906–4913
- Pirrucello SJ, LeBien TW (1986) The human B cell-associated antigen CD24 is a single chain sialoglycoprotein. *J Immunol* (Baltimore, md.: 1950) 136(10):3779–3784
- Tarhriz V et al (2019) Overview of CD24 as a new molecular marker in ovarian cancer. *J Cell Physiol* 234(3):2134–2142. <https://doi.org/10.1002/jcp.27581>
- Barkal AA et al (2019) CD24 signalling through macrophage Siglec-10 is a target for cancer immunotherapy. *Nature* 572(7769):392–396. <https://doi.org/10.1038/s41586-019-1456-0>
- Baumann P et al (2012) CD24 interacts with and promotes the activity of c-src within lipid rafts in breast cancer cells, thereby increasing integrin-dependent adhesion. *Cell Mol Life Sci* 69(3):435–448. <https://doi.org/10.1007/s00018-011-0756-9>
- Kwon MJ et al (2015) CD24 overexpression is associated with poor prognosis in luminal a and triple-negative breast cancer. *PLoS ONE* 10(10):e0139112. <https://doi.org/10.1371/journal.pone.0139112>
- Chan SH et al (2019) Identification of the novel role of CD24 as an oncogenesis regulator and therapeutic target for triple-negative breast cancer. *Mol Cancer Ther* 18(1):147–161. <https://doi.org/10.1158/1535-7163.Mct-18-0292>
- Deng X et al (2017) CD24 Expression and differential resistance to chemotherapy in triple-negative breast cancer. *Oncotarget* 8(24):38294–38308. <https://doi.org/10.18632/oncotarget.16203>
- Jing X et al (2018) CD24 is a potential biomarker for prognosis in human breast carcinoma. *Cell Physiol Biochem Int J Exp Cell Physiol Biochem Pharmacol* 48(1):111–119. <https://doi.org/10.1159/000491667>
- Maliar A et al (2012) Redirected T cells that target pancreatic adenocarcinoma antigens eliminate tumors and metastases in mice. *Gastroenterology* 143(5):1375–1384.e1375. <https://doi.org/10.1053/j.gastro.2012.07.017>
- Sun F et al (2021) Bispecific CAR-T cells targeting both BCMA and CD24: a potentially treatment approach for multiple myeloma. *Blood* 138:2802
- Sun F et al (2017) Engineering a high-affinity humanized anti-CD24 antibody to target hepatocellular carcinoma by a novel CDR grafting design. *Oncotarget* 8(31):51238–51252. <https://doi.org/10.18632/oncotarget.17228>
- Jayaraman J et al (2020) CAR-T design: elements and their synergistic function. *EBioMedicine* 58:102931. <https://doi.org/10.1016/j.ebiom.2020.102931>
- Xu N et al (2021) STING agonist promotes CAR T cell trafficking and persistence in breast cancer. *J Exp Med*. <https://doi.org/10.1084/jem.20200844>
- Liedtke C et al (2008) Response to neoadjuvant therapy and long-term survival in patients with triple-negative breast cancer. *J Clin Oncol* 26(8):1275–1281. <https://doi.org/10.1200/jco.2007.14.4147>
- Zhao Z, Chen Y, Francisco NM, Zhang Y, Wu M (2018) The application of CAR-T cell therapy in hematological malignancies: advantages and challenges. *Acta Pharm Sin B* 8(4):539–551. <https://doi.org/10.1016/j.apsb.2018.03.001>
- Xia L et al (2020) EGFR-targeted CAR-T cells are potent and specific in suppressing triple-negative breast cancer both in vitro and in vivo. *Clin Transl Immunol* 9(5):e01135. <https://doi.org/10.1002/cti2.1135>
- Corti C et al (2022) CAR-T cell therapy for triple-negative breast cancer and other solid tumors: preclinical and clinical progress. *Expert Opin Investig Drugs* 31(6):593–605. <https://doi.org/10.1080/13543784.2022.2054326>
- Tchou J et al (2017) Safety and efficacy of intratumoral injections of chimeric antigen receptor (CAR) T cells in metastatic breast cancer. *Cancer Immunol Res* 5(12):1152–1161. <https://doi.org/10.1158/2326-6066.Cir-17-0189>
- Yamashita N et al (2021) MUC1-C integrates activation of the IFN- $\gamma$  pathway with suppression of the tumor. *J Immunother Cancer* 9:1
- Wei J et al (2018) A novel AXL chimeric antigen receptor endows T cells with anti-tumor effects. *Cell Immunol* 331:49–58
- Chen H et al (2021) CD27 enhances the killing effect of CAR T cells targeting trophoblast cell. *Cancer Immunol Immunother* 70:2059–2071
- Yang XR et al (2009) CD24 is a novel predictor for poor prognosis of hepatocellular carcinoma after surgery. *Clin Cancer Res* 15(17):5518–5527. <https://doi.org/10.1158/1078-0432.Ccr-09-0151>
- He H et al (2015) A novel antibody targeting CD24 and hepatocellular carcinoma in vivo by near-infrared fluorescence imaging. *Immunobiology* 220(12):1328–1336. <https://doi.org/10.1016/j.imbio.2015.07.010>
- Maus MV et al (2013) T cells expressing chimeric antigen receptors can cause anaphylaxis in humans. *Cancer Immunol Res* 1:26–31

33. Lv J et al (2019) Mesothelin is a target of chimeric antigen receptor T cells for treating gastric cancer. *J Hematol Oncol* 12(1):18. <https://doi.org/10.1186/s13045-019-0704-y>
34. Cherkassky L, Hou Z, Amador-Molina A, Adusumilli PS (2022) Regional CAR T cell therapy: an ignition key for systemic immunity in solid tumors. *Cancer Cell* 40(6):569–574. <https://doi.org/10.1016/j.ccell.2022.04.006>
35. Adusumilli PS et al (2014) Regional delivery of mesothelin-targeted CAR T cell therapy generates potent and long-lasting CD4-dependent tumor immunity. *Sci Transl Med* 6(261):261151. <https://doi.org/10.1126/scitranslmed.3010162>
36. Hou AJ, Chen LC, Chen YY (2021) Navigating CAR-T cells through the solid-tumour microenvironment. *Nat Rev Drug Discov* 20(7):531–550. <https://doi.org/10.1038/s41573-021-00189-2>
37. Sun C, Mezzadra R, Schumacher TN (2018) Regulation and function of the PD-L1 checkpoint. *Immunity* 48(3):434–452. <https://doi.org/10.1016/j.immuni.2018.03.014>
38. Cherkassky L et al (2016) Human CAR T cells with cell-intrinsic PD-1 checkpoint blockade resist tumor-mediated inhibition. *J Clin Invest* 126(8):3130–3144. <https://doi.org/10.1172/jci83092>
39. Grosser R, Cherkassky L, Chintala N, Adusumilli PS (2019) Combination immunotherapy with CAR T cells and checkpoint blockade for the treatment of solid tumors. *Cancer Cell* 36(5):471–482. <https://doi.org/10.1016/j.ccell.2019.09.006>
40. Rafiq S et al (2018) Targeted delivery of a PD-1-blocking scFv by CAR-T cells enhances anti-tumor efficacy in vivo. *Nat Biotechnol* 36(9):847–856. <https://doi.org/10.1038/nbt.4195>
41. Choi BD et al (2019) CRISPR-Cas9 disruption of PD-1 enhances activity of universal EGFRvIII CAR T cells in a preclinical model of human glioblastoma. *J Immunother Cancer* 7(1):304. <https://doi.org/10.1186/s40425-019-0806-7>
42. Yu S, Yi M, Qin S, Wu K (2019) Next generation chimeric antigen receptor T cells: safety strategies to overcome toxicity. *Mol Cancer* 18(1):125. <https://doi.org/10.1186/s12943-019-1057-4>
43. Rafiq S, Hackett CS, Brentjens RJ (2020) Engineering strategies to overcome the current roadblocks in CAR T cell therapy. *Nat Rev Clin Oncol* 17(3):147–167. <https://doi.org/10.1038/s41571-019-0297-y>
44. Paszkiewicz PJ et al (2016) Targeted antibody-mediated depletion of murine CD19 CAR T cells permanently reverses B cell aplasia. *J Clin Invest* 126(11):4262–4272. <https://doi.org/10.1172/jci84813>

**Publisher's Note** Springer Nature remains neutral with regard to jurisdictional claims in published maps and institutional affiliations.

Springer Nature or its licensor (e.g. a society or other partner) holds exclusive rights to this article under a publishing agreement with the author(s) or other rightsholder(s); author self-archiving of the accepted manuscript version of this article is solely governed by the terms of such publishing agreement and applicable law.